


Holocene sedimentation in the Hupo Trough of the southwestern East Sea (Japan Sea) and development of the East Korea Warm Current

The Holocene
2021, Vol. 31(7) 1148–1157
© The Author(s) 2021
Article reuse guidelines:
sagepub.com/journals-permissions
DOI: 10.1177/09596836211003238
journals.sagepub.com/home/hol


Boo-Keun Khim,¹  Sunghan Kim,² Yu-Hyeon Park,³ Jongmin Lee,¹ Sangbeom Ha¹ and Kyu-Cheul Yoo²

Abstract

Various sediment properties, such as mean grain size, total organic carbon, total nitrogen, C/N ratio, CaCO₃, and biogenic opal content, were analyzed for a box core (BC02; 45 cm long) and a gravity core (GC02; 628 cm long), which were collected from the western margin of the Hupo Trough located off the eastern coast of Korea. The study area has been affected by the East Korea Warm Current (EKWC), a branch of the Tsushima Warm Current (TWC). The analytical results obtained for BC02 and the upper part of GC02 were in agreement, affirming the core-top preservation of GC02. Based on the corrected calibrated AMS ¹⁴C dates, the sedimentation rate of GC02 changed abruptly at ~8.2 ka from ~4.0–10.2 cm/kyr in the lower part to ~56.6–91.0 cm/kyr in the middle to upper part. This corresponds to the lithologic change from sandy mud to mud sediments showing the mean grain size change from 6.9 to 46.0 μm. Diverse paleoceanographic proxies representing the surface water condition exhibited varying degree of change at ~8.2 ka, after which all the properties remain almost unchanged, implying stable and continuous depositional conditions following the complete development of the EKWC. Furthermore, it indicated that the sediment depositional conditions in the Hupo Trough in response to the EKWC might have stabilized at ~8.2 ka since the opening of the Korea Strait during the Holocene sea level rise. Moreover, microfossil data from previous studies on the establishment of the TWC in the East Sea (Japan Sea) support our interpretation that the sediment properties revealed the Holocene development of the EKWC in the Hupo Trough.

Keywords

geochemical properties, paleoceanography, sea level, sediment deposition, Tsushima Warm Current

Received 1 February 2021; revised manuscript accepted 15 February 2021

Introduction

The eustatic sea level fluctuations by tectonic or glacial forcing have influenced the terrestrial and oceanographic environment. The Bering Strait throughflow connects the Bering Sea of the North Pacific with the Chukchi Sea of the Arctic Ocean. During the last glacial period, a drop in the sea level caused the closure of the Bering Strait, leading to a halt of the Bering Strait throughflow, which controlled the climatic variability in the North Atlantic (e.g. Hu et al., 2012). At the same time, the connection of Asia with Alaska by sea level lowering formed the Bering land bridge (i.e. Beringia), which provided a postulated route of human migration from Asia to America (Goebel et al., 2008). Similar to the Bering Strait region, the East Sea, known as the Japan Sea (hereafter the East Sea), as a marginal sea almost enclosed by the East Asian continent and the Japanese islands, is an exceptionally sensitive to the sea level change (Figure 1(a)).

The East Sea consists of three basins namely the Ulleung Basin, the Yamato Basin, and the Japan Basin. The sea is deeper than 2000 m, and is connected to neighboring seas through shallow straits (Tatarskiy Strait: 12 m, Soya Strait: 55 m, Tsugaru Strait: 130 m, and Korea Strait: 140 m) (Figure 1(a)). The relatively broad (approximately 150 km wide) Korea Strait between the Korean Peninsula and the Japanese islands acts as the main entrance for the Tsushima Warm Current (TWC) which is a branch of the

Kuroshio Current (Figure 1(b)) (Chang et al., 2004). The TWC splits into three branches after flowing through the Korea Strait (Figure 1(b)) (Katoh, 1994). The first branch (i.e. Nearshore Branch: NB) through the eastern channel of the strait roughly follows the 200-m isobath of the continental shelf along the Japanese coast. The second branch (i.e. Offshore Branch: OB) through the western channel of the strait flows along the continental shelf break and slope of the Japanese margin. The third branch, known as the East Korea Warm Current (EKWC), flows along the eastern coast of Korea as a western boundary current.

Glacio-eustatic sea level fluctuations are critical key processes that bring about dramatic environmental shift between the glacial and interglacial periods of the East Sea, because all the straits connecting the East Sea with the neighboring seas are very

¹Department of Oceanography, Pusan National University, Busan, Korea

²Division of Glacial Environment Research, Korea Polar Research Institute, Incheon, Korea

³Marine Research Institute, Pusan National University, Busan, Korea

Corresponding author:

Boo-Keun Khim, Department of Oceanography, Pusan National University, Jangjeon-dong, Geumjeong-gu, Busan 46241, Korea.
Email: bkkhim@pusan.ac.kr

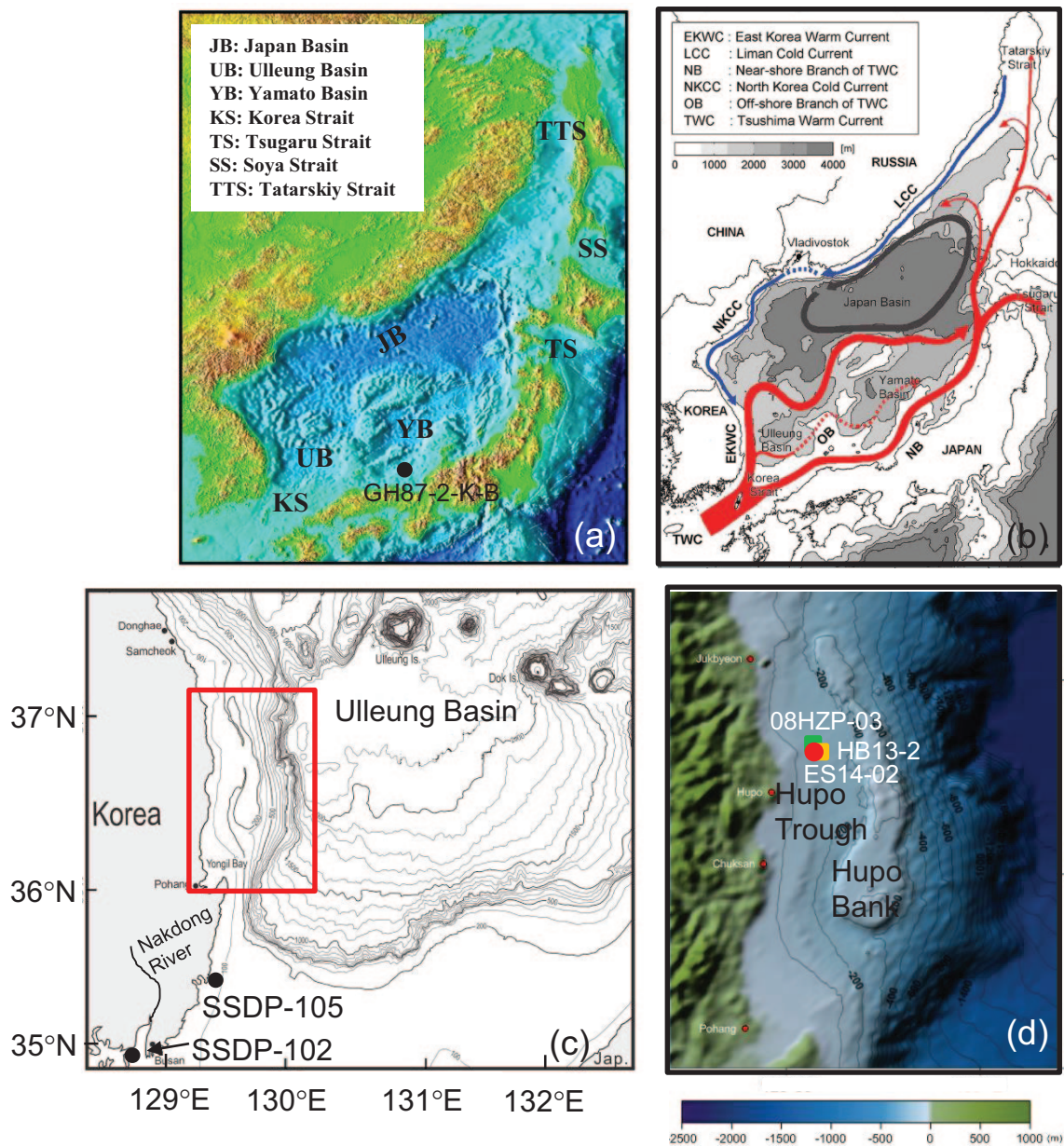


Figure 1. (a) Physiography of the East Sea with the core location of GH87-2-K-B (black circle), (b) surface currents in the East Sea, (c) bathymetry of the Ulleung Basin to show the study area (red box) and the location of cores SSDP-102 and SSDP-105, and (d) bathymetry of the Hupo Trough and the Hupo Bank with the core location of ES14-02 (red circle), 08HWP-03 (green rectangle), and HB13-2 (yellow rectangle).

shallow (Gallagher et al., 2018; Itaki et al., 2004; Khim et al., 2007, 2008, 2009, 2012; Kido et al., 2007; Oba et al., 1991; Tada et al., 1999). The East Sea was almost isolated during the last glacial maximum (LGM; 26.5–19 ka, Clark et al., 2009) when the global sea level was lowered by approximately 120–130 m (Fairbanks, 1989). Thus, the present-day physiography and hydrographic conditions of the East Sea are extremely different from the LGM when the low sea level almost isolated the East Sea from the neighboring seas. For example, such a physiographic constriction prevented the influx of the TWC, which subsequently caused a remarkable change in the sediment deposition due to the hydrographic alteration of seawater properties. As a result, in response to the low sea level position during the last glacial period, the dark laminated mud layers characterized by the high concentration of redox-sensitive elements were deposited on the seafloor at a water depth greater than at least 500 m (Bahk et al., 2000; Crusius et al., 1999; Ikehara et al., 1994; Khim et al., 2008, 2009, 2012).

The TWC disappeared during the LGM due to the subaerial exposure of shallow shelf areas around the Korea Strait (e.g. Park

et al., 2000). During the postglacial period, the TWC began to enter into the East Sea by the Holocene sea level rising. The development of the TWC plays an important role in transporting heat and moisture into the East Sea, leading to a stable climate regime. For example, Gotanda and Yasuda (2008) found that the spatial changes in the biome in southwestern Japan have been dependent on the presence of the TWC since the LGM. The evolution of the TWC after the breaching of the Korea Strait in response to the postglacial sea level rise was revealed mostly by microfossil studies (Domitsu and Oda, 2006, 2008; Itaki et al., 2004; Kim et al., 2000; Koizumi, 1989, 2008; Oba et al., 1991; Takata et al., 2018; Ujiie and Ichikura, 1973). These studies postulated that the initiation of the TWC occurred at about 11–9 ka, and the modern-type establishment was complete at around 9–7 ka.

The high-resolution seismic profiling and sediment coring were conducted extensively on the continental shelf adjacent to the Korea Strait which acts as the gateway of the TWC (e.g. Yoo et al., 2014a, 2014b). Yoo et al. (2014a) revealed that the seismic units of the sedimentary sequence in the continental shelf were

highly correlated with the lithologic units of core SSDP-102 (34°57'2"N, 128°52.9'E, 40 m deep; Kong and Park, 2007) drilled in the inner continental shelf near the Nakdong River estuary. These sedimentary sequences were established in response to the postglacial sea level rise and the sediment supply from the Nakdong River during the development of the TWC. Consequently, the thick accumulation of Holocene sediments in the inner shelf around the Korea Strait indicated that the Nakdong River had played an important role in supplying the fine-grained sediments into the East Sea. Additionally, the EKWC led to the deposition of Nakdong River-derived sediments along the southeastern coast of Korea after the breaching of the Korea Strait during the postglacial sea level rise (Chun et al., 2015; Kong and Park, 2007; Lee et al., 2010).

Among the three branches of the TWC, the evolution of the EKWC flowing along the southeastern coast of Korea has not been studied in detail, compared with the OB and NB. In this study, we document the multi-proxy data of a box core (BC02) and a gravity core (GC02) collected from the western margin of the Hupo Trough in the southwestern East Sea, where the EKWC is dominant. Our results highlighted that the sediment properties of GC02 in the Hupo Trough revealed the depositional history in response to the Holocene sea level rise. Based on the results, we suggest the timing at the complete development of the EKWC similar to the present-day in terms of depositional process in the Hupo Trough.

Study area

The Ulleung Basin occupies the southwestern part of the East Sea (Figure 1(c)). Along the western continental margin of Ulleung Basin, the continental shelf is generally flat and narrow (~20 km wide) with an abrupt and steep continental slope at a water depth of 130–150 m (Figure 1(d)). The upper continental slope comprises a submarine ridge (Hupo Bank) and a depression (Hupo Trough), which are aligned parallel to the shoreline along the eastern coast of Korea (Figure 1(d)). The Hupo Bank is approximately 100 km long and has a relatively flat top at a water depth of 10–200 m. The Hupo Trough, bordered by the Hupo Bank and located on the wide, flat, and shallow (<200 m deep) continental margin, consists of a small sediment depository influenced by the EKWC (Figure 1(b)). Because the Hupo Trough is shallower than ~200 m, the anoxic bottom water was not effective during the last glacial period. For example, the dark laminated mud layer was not observed in the glacial sediments of the 7.4-m-long core 08HZP-03 (36°42.0'N, 129°39.4'E, 195.4 m deep) in the Hupo Trough (Kim et al., 2010).

Active efforts were made to investigate the geological structures in the Hupo Trough (e.g. Yoon et al., 2014), but very few studies involved understanding the sediment cores (Kim et al., 2010; Jun et al., 2014). Kim et al. (2010) reported that the $\delta^{13}\text{C}$ and $\delta^{15}\text{N}$ values of organic matter from core 08HZP-03 divided three intervals; the first (<6 ka) characterized by marine algae, the second (6–10 ka) consisting of a mixture of C_3 land plant and marine/fresh algae, and the third (>10 ka) characterized by C_3 land plants. The sediments of 3.3-m long core HB13-2 (36°42.70'N, 129°42.32'E, 193 m deep) include diverse minerals such as quartz, microcline, orthoclase, albite, and clay minerals (chlorite, kaolinite, illite, and smectite). However, there was not much variation in the mineralogical composition throughout the core, indicating that the sediment source may be limited (Jun et al., 2014).

The Nakdong River, located in southeastern Korea, has a drainage area of approximately 24,000 km² and annually discharges about 6.3×10^{10} tons of freshwater and 10×10^6 tons of sediment (Figure 1(c); Williams et al., 2013). The major discharge (about 71%) of water and sediments occurs during the summer rainy season (Park and Chu, 1991). In general, turbid river plumes formed by the discharged water and sediments were dispersed

into the nearby bay or flow northeastward parallel to the coast (Lee et al., 2006). Consequently, the EKWC transports the river-derived sediments through the Korea Strait into the Ulleung Basin. A distal mud deposit (Korea Strait shelf mud) along the southeastern coast of Korea in a modern-type depositional environment might be formed by shore-parallel sediment transport (Bahk et al., 2004; Chun et al., 2015; Lee et al., 2010).

Materials and methods

A box core (ES14-BC02; 45 cm long, hereafter BC02) and a gravity core (ES14-GC02; 628 cm long, hereafter GC02) were collected at site ES14-02 (36°42.03'N, 129°39.36'E, 189 m deep) located on the western margin of the Hupo Trough during the test cruise of IB Araon in 2014 (Figure 1(d)). The cores were delivered to the laboratory of Korea Polar Research Institute (KOPRI) for preliminary observation, photographs, and sediment sampling for further analyses. A photograph of the sediment slab obtained from the gravity cores was taken at KOPRI. Prior to the laboratory analysis in the Pusan National University, the sediment samples were obtained from BC02 and GC02 at 1 and 2 cm intervals, respectively.

Grain size was analyzed for 14 selected samples using a Laser Diffraction Particle Analyzer Microtrac S3500 at the Korea Institute of Geology and Mineral Resources. For pretreatment prior to the measurement, the organic matter of the dried bulk sediments was removed using a 6% hydrogen peroxide solution. Because of very low CaCO_3 content, CaCO_3 was not removed. Mean grain size and granulometry were calculated using the Gradistat (Blott and Pye, 2001). Total carbon (TC) and total nitrogen (TN) contents were measured at 1 cm interval ($n=45$) for BC02 and at 2 cm intervals ($n=317$) for GC02, using an elemental analyzer (Model Flash 2000). The analytical precision of the instrument expressed as relative standard deviation ($\pm 1\sigma$) was 1%. Total inorganic carbon (TIC) content was measured at 8 cm intervals ($n=80$) for GC02, using a UIC CO_2 Coulometer (Model CM5014). Assuming that all TIC is in the form of CaCO_3 , TIC content is converted to CaCO_3 content as a weight percentage using the multiplying factor 8.333. The analytical error involved in TIC measurement was expressed as one relative standard deviation ($\pm 1\sigma$) and found to be $\pm 1.0\%$. Total organic carbon (TOC) content was calculated by determining the difference between TC and TIC. C/N ratio was calculated by TOC/TN. The biogenic silica content was analyzed at 2–4 cm intervals ($n=163$) for GC02 by the wet alkaline extraction method modified from DeMaster (1981). The relative error of biogenic silica content in sediment samples was less than 1%. The biogenic opal content was calculated by multiplying the biogenic silica content by 2.4 (Mortlock and Froelich, 1989). The analytical data were tabulated in Supplemental Data File.

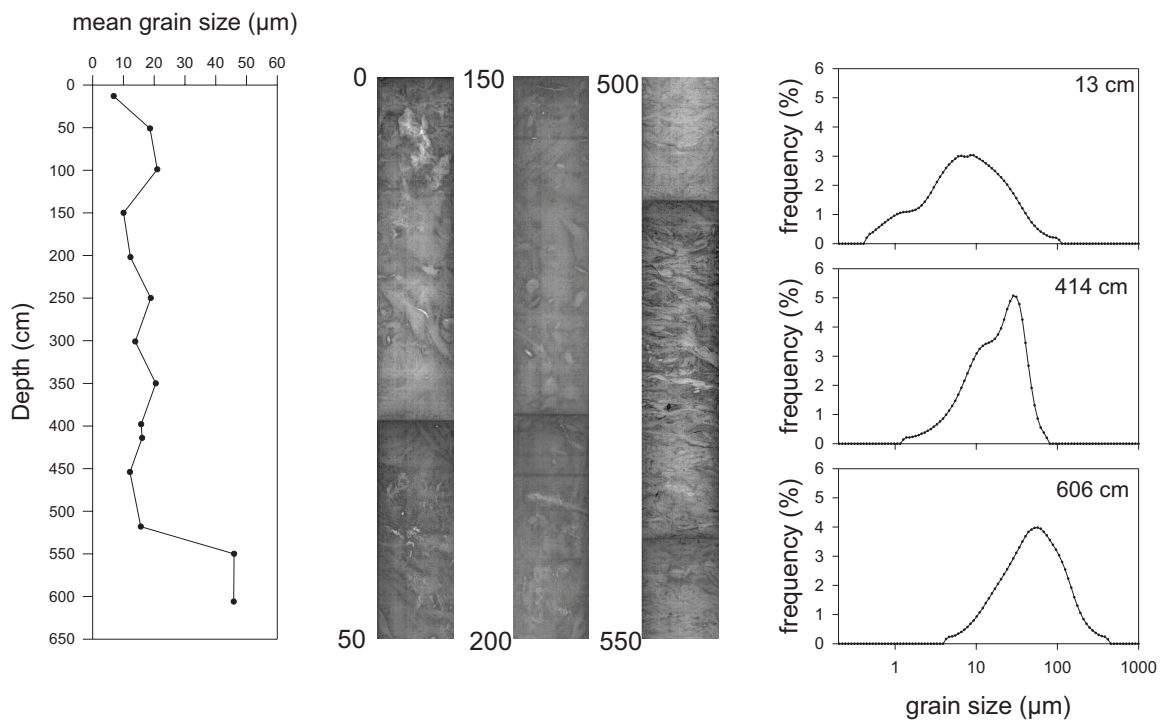
Because foraminiferal tests were rare in GC02, accelerator mass spectrometry (AMS) was operated to determine the abundance of ^{14}C in the acid-insoluble organic matter fraction of the seven bulk sediments at the Rafter Radiocarbon Laboratory, Institute of Geological and Nuclear Sciences (New Zealand). Mixed benthic foraminifera at a depth of 592 cm in GC02 were also dated to provide additional information. Table 1 lists AMS ^{14}C conventional ages (yrBP), which were converted to calibrated calendar year (cal yrBP) with a marine reservoir effect of 400 years (i.e. $\Delta R=0$) (e.g. Kong and Park, 2007) using the CALIB Radiocarbon Calibration Program version 7.1 (Stuiver et al., 2017). In this study, the age unit of “ka” is equivalent to the calibrated age unit of “cal kyr BP.”

Results

Sediments of GC02 consists mostly of bioturbated and homogeneous mud with faintly-laminated mud, and bioturbated sandy mud (Figure 2). Based on the sediment texture, GC02 is divided

Table 1. AMS ^{14}C ages of core ES14-GC02 in the Hupo Trough of the Ulleung Basin in the southwestern East Sea.

Depth (cm)	Conventional ^{14}C age (yrBP)	Error ($\pm 1\sigma$)	$\delta^{13}\text{C}$ (‰)	Calibrated ^{14}C age (cal yrBP)	Corrected calibrated ^{14}C age (cal yrBP)	Material	Lab code
1–2	1167	20	-21.8	706	6	Bulk sediments	NZA60892
154–155	2766	21	-21.4	2492	1792	Bulk sediments	NZA60893
311–312	4073	25	-21.7	4111	3411	Bulk sediments	NZA61034
482–483	6599	27	-21.3	7131	6431	Bulk sediments	NZA60894
526–527	10,387	46	-23.4	11,455	10,755	Bulk sediments	NZA61660
558–559	17,440	95	-23.7	20,547	19,847	Bulk sediments	NZA61661
622–623	31,843	523	-23.5	35,352	34,652	Bulk sediments	NZA61035
592	30,501	362	0.3	34,164		Benthic foraminifera	NZA61075

**Figure 2.** Downcore profile of mean grain size of core GC02, some representative radiographs showing the main sedimentary structures, and three grain size distributions showing the dominant mode change. Upward fining of mean grain size is distinct in the lower part of the core and the mean grain size is almost consistent from the middle to the upper part of the core.

into three lithologic units: the sandy mud from the core-bottom to ~550 cm, the transitional interval from ~550 to ~518 cm, and the mud from ~518 cm to the core-top. Moreover, the transitional interval between the upper and lower lithologic units is characterized by strong bioturbation with the lithologic boundary at 510 cm (Figure 2). Mean grain size of sediments ranged between 6.9 and 46.0 μm , clearly showing the fining-upward trend, which was divided into the lower part from the core-bottom to 550 cm and the middle to upper part from 518 cm to the core-top with a transition from 550 to 518 cm. The mean grain size remains more or less constant (6.9–21.0 μm , mean 15.2 μm) in the middle to upper part of core. The fining-upward change of GC2 was also supported by the grain size distribution that the dominant mode shifts from the coarse to the fine fraction (Figure 2). The mean grain size (6.9 μm) of the upper part (13 cm) of GC02 is almost similar to that ($\sim 8\phi \approx 4 \mu\text{m}$) of nearby core HB13-2 (Jun et al., 2014).

TC and TN contents of the upper part of GC02 were compared with those of BC02 (Supplemental Figure S1), because the top part of the gravity corer was sometimes lost during the core retrieval process, whereas box corer preserved the complete sediment-water interface of the core-top. The variability in the TC and TN contents between the top part of GC02 and BC02 was very similar within a small analytical error range (Supplemental Figure

S1). Moreover, both cores exhibited that TC and TN contents increased slightly and gradually from ~16 cm toward the core-top, confirming that the core-top of GC-02 was rarely missing.

Downcore variations of various geochemical properties (TOC and TN contents, C/N ratio, and CaCO_3 and biogenic opal contents) of GC02, representing the surface water condition, are shown in Figure 3. The variations in the properties follow a pattern similar to the changes in the lithology represented by the mean grain size (Figure 2). There was remarkable change in the sediment properties between the upper and lower units. It is clearly discernible that all the profiles except for the biogenic opal content exhibited nearly no variation above ~500 cm in the upper lithologic unit. Compared with other geochemical properties, there were some fluctuations in the biogenic opal content throughout the core. At ~560 cm, the C/N ratio was the maximum, whereas all the other properties had the minimum values. From the core-bottom to ~560 cm, there were slight decreases in TOC, TN, and biogenic opal contents and moderate decreases in CaCO_3 content, whereas the C/N ratio slightly increased. In contrast, TOC and TN contents increased and C/N ratio decreased distinctly from ~560 to ~500 cm. Consequently, it can be stated that the variations in the C/N ratios and TOC and TN contents were contrary each other in the lower unit. It is worth of note that

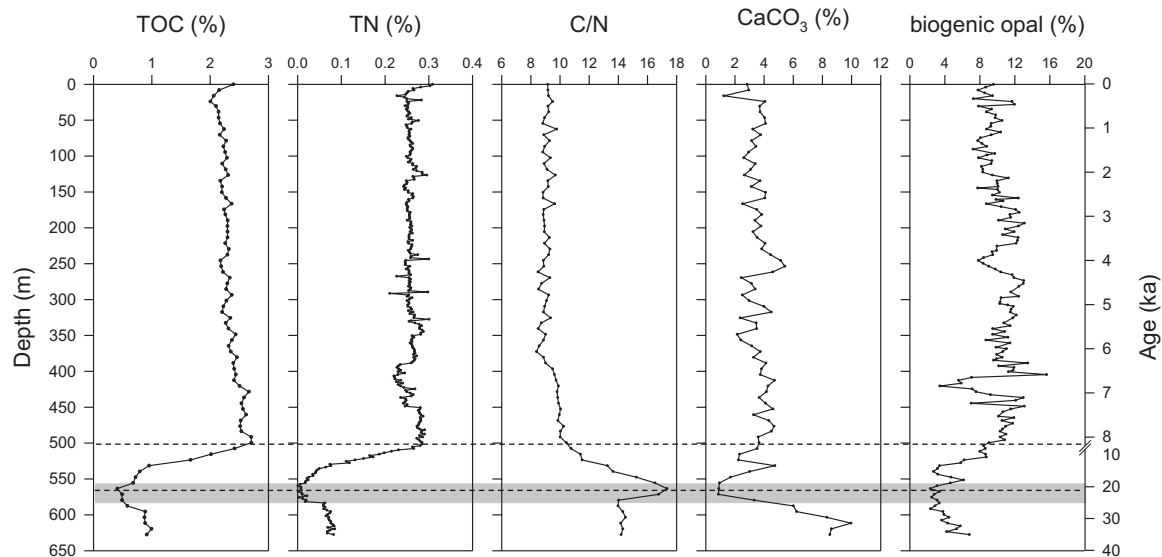


Figure 3. Downcore profiles with depth and time of sediment geochemical properties (total organic carbon (TOC), total nitrogen (TN), TOC/TN (C/N), CaCO_3 , and biogenic opal contents) of core GC02. The variations in these properties were distinct between 500 and 560 cm. There was almost no change in the properties since ~ 8.2 ka. The minimum is marked at the LGM (gray interval).

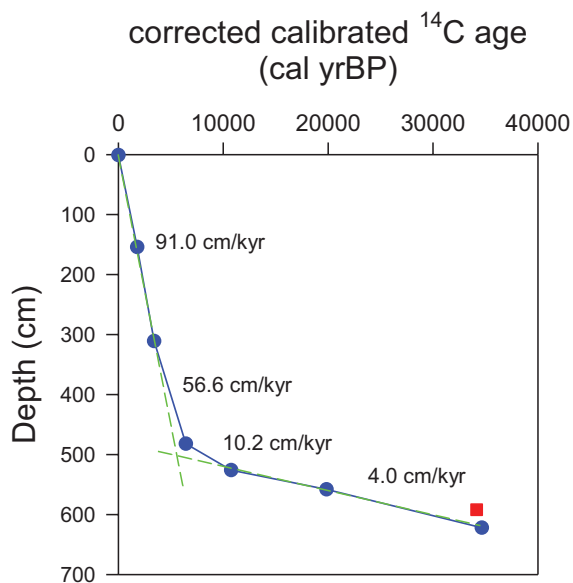


Figure 4. Age-depth relationship of core GC02 (Table 1). Blue dots represent bulk sediments, and the red rectangle represent mixed benthic foraminifera. The change in the sedimentation rate is distinct at ~ 500 cm by green dashed lines. The sediment ages were calculated using the sedimentation rate for each interval.

CaCO_3 and biogenic opal contents also followed the increasing pattern in TOC and TN contents during this interval. Therefore, the lithologic change in terms of mean grain size from 550 to 518 cm in GC02 was reflected by the variation in geochemical properties from 560 to ~ 500 cm.

AMS ^{14}C ages of the bulk sediments and sedimentation rate

The AMS ^{14}C ages of seven bulk sediments in GC02 showed no age reversal (Figure 4), validating a reliable stratigraphic order of sediment deposition. The AMS ^{14}C measurements were performed on the acid-insoluble organic matter of the bulk sediments (Table 1). Because fresh (autochthonous) organic matter is likely to

dissolve in HCl and HNO_3 , the acid-insoluble organic matter could be more affected by old allochthonous (continental) organic matter. Thus, AMS ^{14}C dating of the acid-insoluble organic matter is likely to show an older age than its depositional age. It is noteworthy that the age of core-top (1–2 cm) was 0.7 ka (Table 1), although the core-top of GC02 was well preserved (Supplemental Figure S1). Such an old age of the core-top is mainly due to the local contamination by old continental and marine organic carbon. For example, such type of contamination is very common during the determination of AMS ^{14}C ages of surface sediments in the Antarctic Ocean (e.g. Andrews et al., 1999). Consequently, the local contamination by acid-insoluble organic matter from the sediments containing older carbon is commonly observed during radiocarbon dating, particularly in the shallow marine environment.

In this study, we assumed that the core-top should be the modern, based on the comparison of sediment properties between the top part of gravity corer (GC02) and box corer (BC02) (Supplemental Figure S1). Thus, the local contamination (0.7 kyr) of core-top age was subtracted from the calibrated AMS ^{14}C ages, although the local contamination factor seems different with time. Ikehara (2000) compared AMS ^{14}C ages between the planktonic foraminifera and organic carbon of marine sediments, and reported that AMS ^{14}C ages of organic carbon were older by ~ 1080 – 1790 years than those of planktonic foraminifera. Despite smaller, the local contamination (0.7 kyr) in this study seems close to that by Ikehara (2000). More contamination by old terrestrial carbon might occur during the low sea level condition. However, because we cannot estimate the contamination factor during the low sea level condition in the study area, we applied the uniform factor throughout the time. In addition, the AMS ^{14}C dating of benthic foraminifera measured at 592 cm was 34.2 ka (Table 1). Such an age of benthic foraminifera by 0.5 kyr older than the expected age at the equivalent depth (27.7 ka) may indicate that the shells were reworked. Thus, we did not consider this age information.

Stratigraphic order of sediment deposition in GC02 is reliable due to no age reversal of the AMS ^{14}C ages, although the bulk sediments were used. For the establishment of age model, we calculated the sediment age using the sedimentation rates. Based on the corrected calibrated AMS ^{14}C dates of seven bulk sediments, it was observed that the sedimentation rate was different between the upper and lower units of the core (Figure 5). There was an abrupt change in the sedimentation rate, that is, from very low (~ 4.0 to ~ 10.2 cm/kyr) to very high (~ 56.6 to ~ 91.0 cm/kyr) at

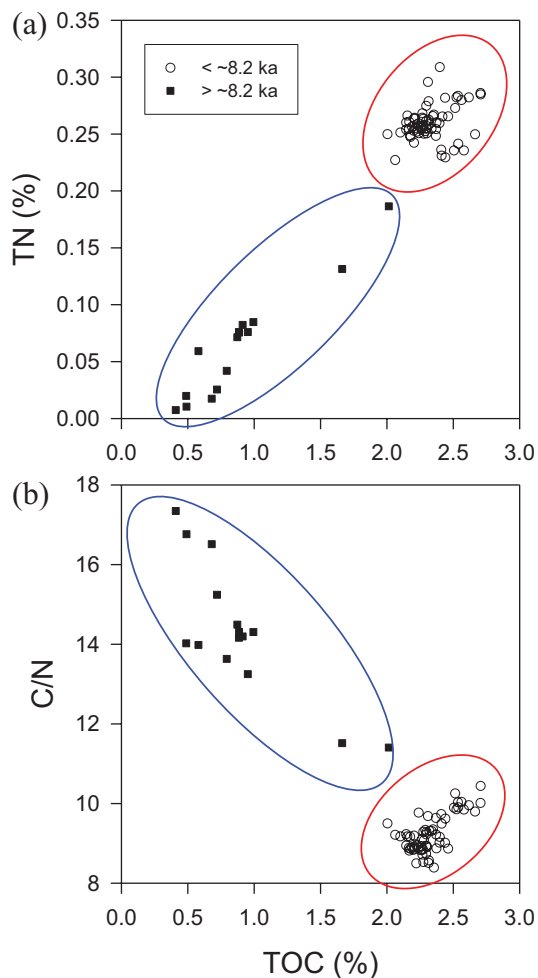


Figure 5. (a) Biplot between TOC and TN contents of core GC02 and (b) biplot between C/N ratio and TOC content of core GC02. Two clusters were distinctly separated by ~ 8.2 ka.

around the lithologic unit boundary (at 510 cm). Such change in the sedimentation rate further confirmed the lithologic division based on the mean grain size and sediment geochemical properties (Figures 2 and 3). With the assumption that the core-top represents the modern and the sedimentation rate is constant between the age points, the calculated ages of the sediments of GC02 were shown in Figure 4. Consequently, the boundary (~ 500 cm) at the geochemical property change was calculated to be about 8.2 ka. Kim et al. (2010) reported that $\delta^{13}\text{C}$ and $\delta^{15}\text{N}$ values of organic matter changed abruptly at 4.75 m depth in core 08HZIP-03 in the Hupo Trough (Figure 1) which is younger than 10.6 ka dated at 5.11 m in 08HZIP-03. Thus, the boundary of organic matter isotopes in 08HZIP-03 may correspond to that of geochemical properties in GC02.

Discussion

Detrital sediment transport changes associated with onset of the EKWC

The very low sedimentation rate (~ 4.0 cm/kyr) observed in the lower part of GC02 confirmed that the sediment delivery was extremely limited during the last glacial period (Figure 4). Although the Hupo Trough is located offshore near the eastern coast of Korea (Figure 1(d)), the supply of terrestrial sediments from Korea is limited because most streams are short and small, and the sediments are deposited in the shallow inner continental shelf (Chough et al., 2000). The sediments deposited in the Hupo Trough might be mainly transported by oceanic current (i.e. the

EKWC), although aeolian processes seem to contribute to a certain extent. Based on the sediment geochemistry, Um et al. (2017) reported that the provenance of fine-grained sediments on the southwestern slope of the Ulleung Basin was also the Nakdong River in addition to Chinese rivers. The mineralogical analyses of sediments in the Hupo Trough showed that the mineral composition of the Holocene sediments was consistent (Jun et al., 2014), confirming that there was no significant change in the sediment provenance. Thus, the conditions near the Korea Strait in response to the sea level position are critical to the supply of sediments from the Nakdong and Chinese rivers to the southern Ulleung Basin and the Hupo Trough by the EKWC.

Bahk et al. (2004) reported that there was a significant increase from 15 to 10 ka in the detrital $\text{SiO}_2/\text{Al}_2\text{O}_3$ and $\text{TiO}_2/\text{Al}_2\text{O}_3$ ratios and silt/clay ratios in the southern margin of the Ulleung Basin during the last deglaciation. It is attributed to the substantial increases in the hemipelagic fluxes particularly associated with the formation of the beach-shore complex during the early stage of the postglacial transgression. However, the shore-parallel sediment transport by the EKWC through the Korea Strait might be ineffective because of the decreased seawater flux governed by a substantial lowering in the sea level during the last deglaciation. Holocene sedimentation rates of GC02 were significantly different before ~ 8.2 ka ($< \sim 10.2$ cm/kyr) and after ~ 8.2 ka (~ 56.6 to ~ 91.0 cm/kyr) (Figure 4). The abrupt change in the sedimentation rate corresponds to the shift in the variation pattern of geochemical properties and lithologic division. Remarkably, sediment properties except for the biogenic opal content were generally constant since ~ 8.2 ka (Figure 3), as was the mean grain size (Figure 2). These features clearly indicated that the depositional conditions in the Hupo Trough might have changed at ~ 8.2 ka.

Productivity changes associated with onset of the EKWC

Since the LGM characterized by the minimum values of TOC, TN, and CaCO_3 , and biogenic opal contents, these geochemical properties increased gradually until ~ 8.2 ka (Figure 3). Such a gradual increase in TOC, TN, and biogenic opal contents implied that the surface water properties were altered, leading to higher primary production presumably due to the warmer seawater and rising sea level. A slightly higher CaCO_3 content ($\sim 10\%$) during the last glacial period is typical of the East Sea (e.g. Oba and Pedersen, 1999). Although the geochemical properties depend on the grain size of sediments, their increases in the Hupo Trough were more affected by the surface water production rather than the grain size effect because the increasing patterns are different among the geochemical properties. It is also noteworthy that, since ~ 8.2 ka, these proxies of surface water production seemed to remain almost constant even under high sedimentation rates (Figure 3). The quasi-cyclic variations in the biogenic opal content during the last 8 kyr were significantly different compared with the variations in other sediment properties of GC02. The diatom, *Fragilariopsis doliolus*, has been regarded as an indicator species for the TWC (Koizumi, 1989). The variations in biogenic opal content during the middle to late-Holocene may be attributed to the degree of diatom production in surface waters of the Hupo Trough with the changes in the strength of the EKWC. This pattern was similar to the variations in the diatom temperature index and abundance of *F. doliolus* with the change in the strength of the TWC in the East Sea (Khim et al., 2005; Koizumi, 1989; Koizumi et al., 2006).

TOC content of bulk sediments of GC02 is influenced by a mixture of sinking particles from the surface water and lateral transport from the nearby land (Stein, 1991). The degree of primary production in the shallow marine environment is the major factor governing TOC content of bulk sediments, assuming that the degree of degradation of the organic matter during sinking

within the water column and on the seafloor remains the same. The biplot between TOC and TN contents displays two separate clusters of TOC and TN contents: one before ~8.2 ka and another after ~8.2 ka, despite the transition at ~8.2 ka (Figure 5(a)). The samples after ~8.2 ka were characterized by higher TOC and TN contents, in addition to higher biogenic opal content (Figure 4), than those before ~8.2 ka. Although the correlation between TOC and TN contents showed similar slopes for the two clusters, the relationships between the clusters and variables were significantly different (Figure 5(a)). The samples before ~8.2 ka showed negligible TN content, which may be attributed to either the selective degradation of nitrogen compounds during the postdeposition or degradation of different compounds of organic matters before ~8.2 ka.

C/N ratio of bulk sediments has been used to differentiate the origin of organic carbon (Hedges and Parker, 1976; Meyers, 1994). C/N ratios of the samples before ~8.2 ka were much higher than those after ~8.2 ka, indicating the greater contribution of terrestrial organic matter before ~8.2 ka (Figure 5(b)). Moreover, the correlation between C/N ratio and TOC content of the two temporal domains was contrary each other (Figure 5(b)). It may indicate that the depositional environment of the organic matter during these two periods was different. Prior to ~8.2 ka, the Hupo Trough was dominated by more terrestrial-derived organic matter whereas more marine organic matters dominated the Hupo Trough after ~8.2 ka. Biomarker and $\delta^{13}\text{C}$ and $\delta^{15}\text{N}$ values of organic matter in the surface sediments of the East Sea revealed the surface water conditions, despite the lateral contribution to the deeper site (Khim et al., 2018; Park et al., 2019). Kim et al. (2010) reported that $\delta^{13}\text{C}$ and $\delta^{15}\text{N}$ values of organic matter in core 08HWP-03 were low before 10.6 ka and high after 6.0 ka, and an environmental condition might be changed sometime between 6.0 and 10.6 ka. Thus, the oceanographic conditions affected by the EKWC in the Hupo Trough may gradually change after the LGM, reaching equilibrium condition at ~8.2 ka.

Onset timing of the EKWC and development of the TWC system

Microfossil studies have revealed the onset timing of the TWC in the East Sea after the breaching of the Korea Strait in response to the postglacial rise in sea level (Domitsu and Oda, 2006, 2008; Itaki et al. 2004; Kim et al., 2000; Koizumi, 1989, 2008; Oba et al., 1991; Takata et al., 2018; Ujiie and Ichikura, 1973). Ujiie and Ichikura (1973) reported that the TWC began to flow at ~11 ka based on the coiling-direction shift of planktonic foraminifera (*Neogloboquadrina pachyderma*). The appearance of *F. doliolus*, which is indicative of the TWC, occurred at 10–9 ka (Koizumi, 1989). Oba et al. (1991) confirmed that the TWC began to flow at ~10 ka, based on the appearance of *F. doliolus*, the change in coiling direction of *N. pachyderma*, and prevalent occurrence of warm-water microfossil species. Moreover, they suggested that the modern-type TWC was established since ~8.2 ka. Based on the predominance of *Cycladophora davisiana* and the absence of *Actinomma boreale/leptoderma* Group, Itaki et al. (2004) suggested that active deep-water formation took place in response to the TWC inflow during the early Holocene (11–9 ka). On the other hand, Kim et al. (2000) reported that the dextrally-coiled *N. pachyderma* appeared in the Ulleung Basin since ~8.0 ka, and the TWC was established by ~6.6 ka.

Koizumi (2008) proposed that the relative abundance of *F. doliolus* represented the first occurrence of the TWC at 8–8.5 ka in the southern part and at 7.5 ka in the northern part of the East Sea. Domitsu and Oda (2006) reported that warm-water planktonic foraminifera (*Globigerinoides ruber*, *N. dutertrei*, *Pulleniatina obliquiloculata*, *G. tenellus*, and *Globigerinita glutinata*) appeared since 9.3 ka, and *N. incompta* was dominant at 7.3 ka. Recently, Takata et al. (2018) found that there was a decrease

from 11.5 to 7 ka in the accumulation of benthic foraminifera, and warm-water planktonic foraminifera commonly occurred at ~9–7 ka. Their results implied that the TWC was initiated before 9.3 ka, and the establishment of modern-type TWC was stabilized before 7.3 ka. Although there has been no microfossil study on the initiation of the EKWC, the timing of its onset can be similarly estimated. Thus, these previous microfossil studies verify that the development of the EKWC expressed in terms of depositional conditions might have been completed at ~8.2 ka.

Based on microfossil studies (Domitsu and Oda, 2006, 2008; Itaki et al. 2004; Kim et al., 2000; Koizumi, 1989, 2008; Oba et al., 1991; Takata et al., 2018; Ujiie and Ichikura, 1973), it can be stated that the TWC appeared in the East Sea after ~9.3 ka at the latest. Because the glaci-eustatic sea level was still lower than ~20 m below the present-day sea level at that time (Fairbanks, 1989), the TWC might have been the proto-type different from the modern-type. According to the abrupt change observed in the sedimentation rate and the significant increase in abundance of *Pulleniatina obliquiloculata* in the outer continental shelf of the Korea Strait, Lim et al. (2006) suggested that the coastal water stage terminated at ~7.0 ka when the TWC began to flow into the East Sea. The sedimentological study by Nishida and Ikehara (2013) off Fukuoka in the Korea Strait proposed that the influence of the TWC on the depositional environment was established after 8.4 ka. Moreover, based on the evaluation of warm-water benthic foraminifera in the Nakdong River Delta, Takata et al. (2016) suggested that the TWC was intensified at ~8 ka. Accordingly, the sediment transport and deposition by the TWC in the Korea Strait might have reached present-day levels since ~8.4 ka.

Figure 6 illustrates the relationship between the sediment deposition and the occurrence of microfossils, in terms of TOC and $\delta^{13}\text{C}_{\text{org}}$, representing the presence of the TWC. The TOC content of GC02 remained almost constant after ~8.2 ka (Figure 6(a)), indicating continuous and uniform deposition of organic matter under the present-day oceanographic conditions in the Hupo Trough. Kong and Park (2007) reported a similar depositional feature at SSDP-105 (35°22.2'N, 129°29.0'E, 79 m deep) located in the distal mud deposit along the southeastern coast of Korea (Figure 6(b)). TOC contents and $\delta^{13}\text{C}_{\text{org}}$ values were generally constant after 7.9 ka, at which the sediment lithology changed abruptly from muddy sand to mud similar to GC02. It reflected that the present-day stable depositional conditions in the Hupo Trough were similarly established, despite a little delay due to the further northward site. In addition, the major discrepancy between the two depositional sites is that the location of SSDP-105 was greatly influenced by the Nakdong River-derived sediments. The sedimentation rate (~3.6 m/kyr) since 7.9 ka at SSDP-105 is more than four to six times that (~56.6 to ~91.0 cm/kyr) since ~8.2 ka. Domitsu and Oda (2008) reported that *N. incompta*, which represents the TWC, first occurred at 9.3 ka along the path of the NB (Figure 6(c)). However, a rapid increase in *N. incompta* abundance began at ~8.0 ka. Hence, the estimated time (~8.2 ka) based on the sediment properties by which the EKWC was established in the Hupo Basin, is reasonably acceptable.

Conclusions

The East Sea has experienced drastic environmental and oceanographic changes between the glacial and interglacial periods, as the sea level fluctuations led to different physiographic configurations and subsequent hydrographic conditions. One of the remarkable oceanographic changes is the initiation and establishment of the TWC (i.e. the EKWC, OB, and NB), which plays an important role in transporting heat and nutrients during the rise in sea level. The Holocene sediments of GC02, collected from the Hupo Trough, provided distinct information on the establishment of the EKWC in terms of present-day sediment depositional processes.

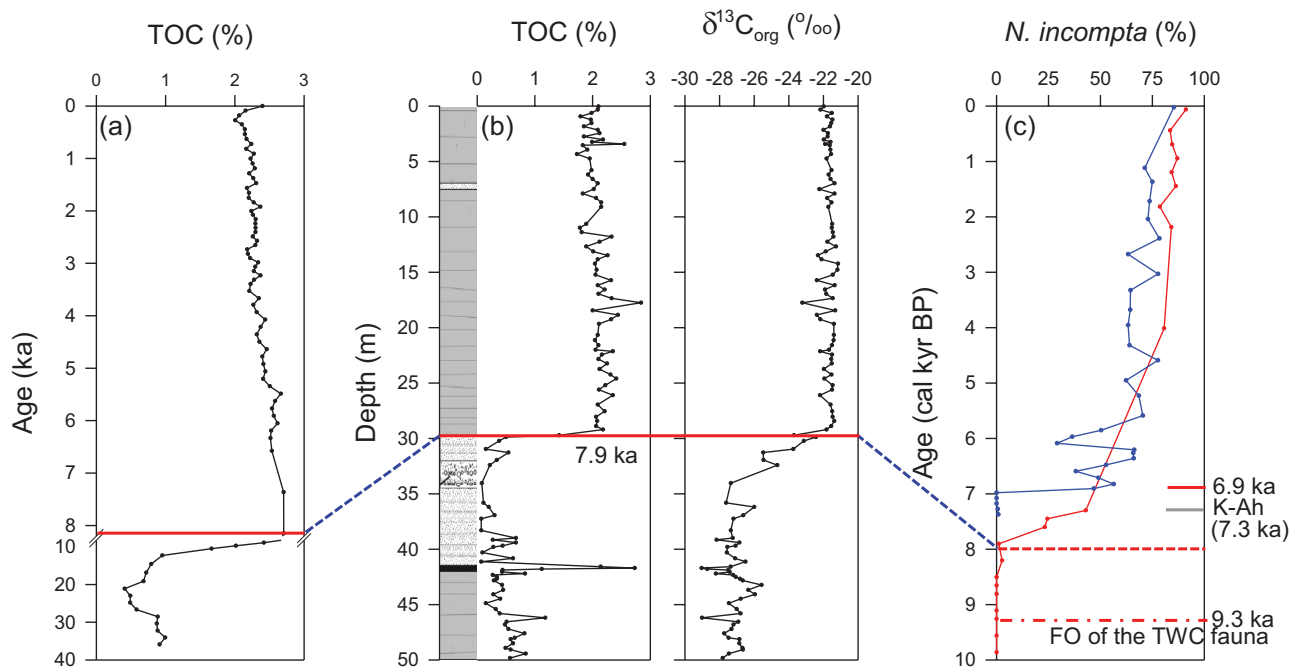


Figure 6. Profiles showing (a) variation in TOC content of core GC02, (b) variations in TOC content and $\delta^{13}\text{C}_{\text{org}}$ value of core SSDP-105 (Kong and Park, 2007), and (c) variation in microfossil abundance (*N. incompta*) of cores GH87-2-K-B (red: Domitsu and Oda, 2006) and KT98-17 P-I (blue: Domitsu and Oda, 2008).

Distinct change among the properties occur at the similar time (~7.9 to ~8.2 ka) for all the cores.

FO: first occurrence; TWC: Tsushima Warm Current.

All the sedimentary features, including sediment lithology, sedimentation rate, mean grain size, geochemical properties, substantiate the evolution of the EKWC by showing an abrupt change in the features at ~8.2 ka and subsequent consistency thereafter. Previous data on microfossils and other geochemical properties in the East Sea support our conclusion that the present-day EKWC, expressed in terms of the sediment transport and depositional conditions, was stabilized at ~8.2 ka.

Acknowledgements

The captain, crew, and all onboard researchers are thanked for core sampling during the test cruise of IB Araon in 2014. We thank greatly anonymous reviewers and editor for their helpful comments and encouragements during the revision of the manuscript. We appreciate Dr. C.H. Kim (KIOST) for providing the figure of study area.

Funding

The author(s) disclosed receipt of the following financial support for the research, authorship, and/or publication of this article: This study was carried out by the National Research Foundation of Korea (2016R1D1A1B03934308, 2019R1A2C1007701) and partly by KOPRI project (PE21090).

ORCID iD

Boo-Keun Khim  <https://orcid.org/0000-0002-0229-7990>

Supplemental material

Supplemental material for this article is available online.

References

- Andrews JT, Domack EW, Cunningham WL et al. (1999) Problems and possible solutions concerning radiocarbon dating of surface marine sediments, Ross Sea, Antarctica. *Quaternary Research* 52: 206–216.
- Bahk JJ, Chough SK and Han SJ (2000) Origin and paleoceanographic significance of laminated muds from the Ulleung Basin, East Sea (Sea of Japan). *Marine Geology* 16: 459–477.
- Bahk JJ, Han SJ and Khim BK (2004) Variations of terrigenous sediment supply to the southern slope of the Ulleung Basin, East/Japan Sea since the Last Glacial Maximum. *Geosciences Journal* 8: 381–390.
- Blott SJ and Pye K (2001) GRADISTAT: A grain size distribution and statistics package for the analysis of unconsolidated sediments. *Earth Surface Processes and Landforms* 26: 1237–1248.
- Chang KI, Teague WJ, Lyu SJ et al (2004) Circulation and currents in the southwestern East/Japan Sea: Overview and review. *Progress in Oceanography* 61: 105–156.
- Chough SK, Lee HJ and Yoon SH (2000) *Marine Geology of Korean Seas*, 2nd edn. Amsterdam: Elsevier.
- Chun JH, Kim Y, Bahk JJ et al. (2015) Late-Holocene distal mud deposits off the Nakdong delta, SE Korea: Evidence for shore-parallel sediment transport in a current-dominated setting. *Geo-Marine Letters* 35: 475–485.
- Clark PU, Dyke AS, Shakun JD et al. (2009) The last glacial maximum. *Science* 325: 710–714.
- Crusius J, Pedersen TF, Calvert SE et al. (1999) A 36 kyr geochemical record from the Sea of Japan of organic matter flux variations and changes in intermediate water oxygen concentrations. *Paleoceanography* 14: 248–259.
- DeMaster DJ (1981) The supply and accumulation of silica in the marine environment. *Geochimica et Cosmochimica Acta* 5: 1715–1732.
- Domitsu H and Oda M (2006) Linkages between surface and deep circulations in the southern Japan Sea during the last 27,000 years: Evidence from planktic foraminiferal assemblages and stable isotope records. *Marine Micropaleontology* 61: 155–170.
- Domitsu H and Oda M (2008) Holocene influx of the Tsushima Current into the Japan Sea signaled by spatial and temporal changes in *Neogloboquadrina incompta* distribution. *The Holocene* 18: 345–352.
- Fairbanks RG (1989) A 17,000-year glacio-eustatic sea level record: Influence of glacial melting rates on the Younger Dryas event and deep-ocean circulation. *Nature* 342: 637–642.
- Gallagher SJ, Sagawa T, Henderson A et al. (2018) East Asian monsoon history and paleoceanography of the Japan Sea over

- the last 460,000 years. *Paleoceanography and Paleoclimatology* 33: 683–702.
- Goebel T, Waters MR and Rourke DH (2008) The late Pleistocene dispersal of modern humans in the Americas. *Science* 319: 1497–1502.
- Gotanda K and Yasuda Y (2008) Spatial biome changes in south-western Japan since the Last Glacial Maximum. *Quaternary International* 184: 84–93.
- Hedges JI and Parker PL (1976) Land-derived organic matter in surface sediments from the Gulf of Mexico. *Geochimica et Cosmochimica Acta* 40: 1019–1029.
- Hu A, Meehl GA, Han W et al. (2012) Role of the Bering Strait on the hysteresis of the ocean conveyor belt circulation and glacial climate stability. *Proceedings of National Academy of Science* 109: 6417–6422.
- Ikehara K (2000) Comparison of radiocarbon ages of planktonic foraminifera and bulk organic carbon in marine sediments. *Bulletin of Geological Survey of Japan* 51: 299–307. (in Japanese with English abstract)
- Ikehara K, Kikkawa K, Katayama H et al. (1994) Late Quaternary paleoceanography of the Japan Sea; a tephrochronological and sedimentological study. In: *Proceedings of 29th International Geological Congress, Part B*, Utrecht, The Netherlands: VSP, pp.229–235.
- Itaki T, Ikehara K, Motoyama I et al. (2004) Abrupt ventilation changes in the Japan Sea over the last 30 ky: Evidence from deep-dwelling radiolarians. *Palaeogeography Palaeoclimatology Palaeoecology* 208: 263–278.
- Jun CP, Kim CH, Kim Y et al. (2014) Paleoenvironmental reconstruction of the Hupo Basin using grain size and mineral analysis. *Journal of Mineralogical Society of Korea* 27: 159–168. (in Korean with English abstract)
- Katoh O (1994) Structure of the Tsushima Current in the south-western Japan Sea. *Journal of Oceanography* 50: 317–338.
- Khim BK, Bahk JJ, Hyun S et al. (2007) Late Pleistocene dark laminated mud layers from the Korea Plateau, western East Sea/Japan Sea, and their paleoceanographic implications. *Palaeogeography Palaeoclimatology Palaeoecology* 247: 74–87.
- Khim BK, Ikehara K and Irino T (2012) Orbital- and millennial-scale paleoceanographic changes in the north-eastern Japan Basin, East Sea/Japan Sea during the late Quaternary. *Journal of Quaternary Science* 27: 328–335.
- Khim BK, Ikehara K and Shin Y (2005) Unstable Holocene climate in the northeastern East Sea (Sea of Japan): Evidence from a diatom record. *Palaeogeography Palaeoclimatology Palaeoecology* 216: 251–265.
- Khim BK, Otosaka S, Park KA et al. (2018) $\delta^{13}\text{C}$ and $\delta^{15}\text{N}$ values of sediment-trap particles in the Japan and Yamato Basins and comparison with the core-top values in the East/Japan Sea. *Ocean Science Journal* 53: 17–29.
- Khim BK, Park YH, Bahk JJ et al. (2008) Spatial and temporal variation of geochemical properties and paleoceanographic implications in the South Korea Plateau (East Sea) during the late Quaternary. *Quaternary International* 176/177: 46–61.
- Khim BK, Tada R, Park YH et al. (2009) Correlation of TL layers for the synchronous paleoceanographic events in the East Sea (Sea of Japan) during the Late Quaternary. *Geosciences Journal* 13: 113–120.
- Kido Y, Minami I, Tada R et al. (2007) Orbital-scale stratigraphy and high-resolution analysis of biogenic components and deep water oxygenation conditions in the Japan Sea during the last 640 kyrs using XRF microscanner. *Palaeogeography Palaeoclimatology Palaeoecology* 247: 32–49.
- Kim JH, Park MH, Kong GS et al. (2010) Geochemical results and implication of the organic matter in the Holocene sediments from the Hupo Basin. *Economic and Environmental Geology* 43: 1–12. (in Korean with English abstract)
- Kim JM, Kennett JP, Park BK et al. (2000) Paleoceanographic change during the last deglaciation, East Sea of Korea. *Paleoceanography* 15: 254–266.
- Koizumi I (1989) Holocene pulses of diatom growths in the warm Tsushima Current in the Japan Sea. *Diatom Research* 4: 55–68.
- Koizumi I (2008) Diatom-derived SSTs (Td' ratio) indicate warm seas off Japan during the middle Holocene (8.2–3.3 kyr BP). *Marine Micropaleontology* 69: 263–281.
- Koizumi I, Tada R, Narita H et al. (2006) Paleoceanographic history around the Tsugaru Strait between the Japan Sea and the Northwest Pacific Ocean since 30 cal kyr BP. *Palaeogeography Palaeoclimatology Palaeoecology* 232: 36–52.
- Kong GS and Park SC (2007) Paleoenvironmental changes and depositional history of the Korea (Tsushima) Strait since the LGM. *Journal of Asian Earth Sciences* 29: 84–104.
- Lee GH, Kim DC, Park MK et al. (2010) Internal reflection pattern of Korea Strait shelf mud (Nakdong River subaqueous delta) off southeast Korea and implications for Holocene relative base-level change. *Island Arc* 19: 71–85.
- Lee HJ, Wang YP, Chu YS et al. (2006) Suspended sediment transport in the coastal area of Jinhae Bay-Nakdong estuary, Korea Strait. *Journal of Coastal Research* 22: 1062–1069.
- Lim DI, Kang S, Yoo HS et al. (2006) Late Quaternary sediments on the outer shelf of the Korea Strait and their paleoceanographic implication. *Geo-Marine Letters* 26: 287–296.
- Meyers PA (1994) Preservation of elemental and isotopic source identification of sedimentary organic matter. *Chemical Geology* 114: 289–302.
- Mortlock RA and Froelich PN (1989) A simple method for the rapid determination of biogenic opal in marine sediments. *Deep-Sea Research* 36: 1415–1426.
- Nishida N and Ikehara K (2013) Holocene evolution of depositional processes off southwest Japan: Response to the Tsushima Warm Current and sea-level rise. *Sedimentary Geology* 290: 138–148.
- Oba T and Pedersen T (1999) Paleoclimatic significance of eolian carbonates supplied to the Japan Sea during the last glacial maximum. *Paleoceanography* 14: 34–41.
- Oba T, Kato M, Kitazato H et al. (1991) Paleoenvironmental changes in the Japan Sea during the last 85,000 years. *Paleoceanography* 6: 499–518.
- Park SC and Chu KS (1991) Dispersal pattern of river-derived fine-grained sediment on the inner shelf of the Korea Strait. In: Takano K (ed.) *Oceanography of Asian Marginal Seas*. Amsterdam: Elsevier, pp.231–240.
- Park SC, Yoo DG, Lee CW et al. (2000) Last glacial sea-level changes and paleogeography of the Korea (Tsushima) Strait. *Geo-Marine Letter* 20: 64–71.
- Park YH, Kim HJ, Son JW et al. (2019) Biomarker-based seawater temperatures of winter sinking particles and core-top sediment in the Ulleung Basin of the East Sea. *Ocean Science Journal* 54: 487–495.
- Stein R (1991) *Accumulation of Organic Carbon in Marine Sediments*. Berlin: Springer-Verlag, p. 217.
- Stuiver M, Reimer PJ and Reimer RW (2017) CALIB 7.1 [WWW program] Available at: <http://calib.org> (accessed September 2017).
- Tada R, Irino T and Koizumi I (1999) Land-ocean linkages over orbital and millennial timescales recorded in late Quaternary sediments of the Japan Sea. *Paleoceanography* 14: 236–247.
- Takata H, Itaki T, Ikehara K et al. (2018) Correlation between faunal transitions of benthic foraminifera and ballasting of particulate organic carbon by siliceous plankton during the Holocene off San-in district, southwestern Japan. *The Holocene* 28: 444–454.

- Takata H, Khim BK, Cheong D et al. (2016) Holocene benthic foraminiferal faunas in coastal deposits of the Nakdong River delta (Korea) and Izumo Plain (Japan). *Quaternary International* 392: 13–24.
- Ujiie H and Ichikura M (1973) Holocene to uppermost Pleistocene planktonic foraminifers in a piston core from off San'in district, Sea of Japan. *Transactions and Proceedings of Palaeontological Society of Japan* 91: 137–150. (in Japanese with English abstract)
- Um IK, Choi MS, Bahk JJ et al. (2017) Provenance of late Quaternary sediments on the southwestern slope of the Ulleung Basin, East/Japan Sea. *Quaternary International* 459: 153–164.
- Williams JR, Dellapenna TM and Lee G (2013) Shifts in depositional environments as a natural response to anthropogenic alterations: Nakdong Estuary, South Korea. *Marine Geology* 343: 47–61.
- Yoo DG, Kim SP, Chang TS et al. (2014a) Late Quaternary inner shelf deposits in response to late Pleistocene-Holocene sea level changes: Nakdong River, SE Korea. *Quaternary International* 344: 157–169.
- Yoo DG, Kim SP, Lee CW et al. (2014b) Late Quaternary transgressive deposits in a low-gradient environmental setting: Korea Strait shelf, SE Korea. *Quaternary International* 344: 143–155.
- Yoon SH, Sohn YK and Chough SK (2014) Tectonic, sedimentary, and volcanic evolution of a back-arc basin in the East Sea (Sea of Japan). *Marine Geology* 352: 70–88.